Res Chem Intermed
https://doi.org/10.1007/s11164-017-3235-6

Novel 1,8-naphthalimide dye for multichannel sensing of H^+ and Cu^{2+}

Yufen Chen[1,2] · Tengxuan Tang[1,2] · Yuhua Chen[3] · Dongmei Xu[1,2]

Received: 22 September 2017 / Accepted: 11 December 2017

Abstract A novel 1,8-naphthalimide dye with simple structure has been produced by a facile synthetic method for colorimetric and fluorescent sensing of H^+ and Cu^{2+}. In CH_3CN/H_2O (1/1, v/v), the dye could monitor H^+ using dual channels (ratiometric absorbance and fluorescence intensity change) from pH 6.2 to 12.0. Meanwhile, in the pH range of 1.9–5.2, the dye could also be used to detect Cu^{2+} using triple channels [ultraviolet–visible (UV–Vis) absorption, fluorescence intensity reduction, as well as fluorescence blueshift]. The detection limits for Cu^{2+} evaluated by colorimetric and fluorescent titration were 6.10×10^{-7} and 2.62×10^{-7} M, respectively. The dye exhibited specific selectivity and sensitivity for H^+ and Cu^{2+} over various coexisting metal ions. Moreover, the sensing mechanism of the dye for H^+ and Cu^{2+} was carefully examined.

Keywords 1,8-Naphthalimide · Colorimetric sensor · Fluorescent sensor · H^+ · Cu^{2+}

Electronic supplementary material The online version of this article (https://doi.org/10.1007/s11164-017-3235-6) contains supplementary material, which is available to authorized users.

✉ Yuhua Chen
chenyh@suda.edu.cn

✉ Dongmei Xu
xdm.sd@163.com

[1] College of Chemistry, Chemical Engineering and Materials Science, Soochow University, No. 199 Ren-ai Road, Suzhou Industrial Park, Suzhou 215123, Jiangsu, People's Republic of China

[2] Jiangsu Key Laboratory of Advanced Functional Polymer Design and Application, Soochow University, Suzhou 215123, Jiangsu, People's Republic of China

[3] College of Pre-clinical Medical and Biological Science, Soochow University, Suzhou 215123, People's Republic of China

Published online: 08 January 2018

Introduction

H^+ and Cu^{2+} are important species in environmental and biological systems. H^+ participates in many physiological processes such as enzymatic activities and ion transport [1], and controls pH-driven switching [2], while destruction of copper homeostasis is implicated in a number of diseases. Copper deficiency can cause bone fragility, cardiovascular disorders, subcutaneous bleeding, and other symptoms, while excessive levels of copper can harm the liver and induce Wilson's disease or gastrointestinal disease [3, 4]. Therefore, development of easier and faster methods for detection of H^+ and Cu^{2+} remains an imperative task.

Spectral sensing has become a promising strategy due to its easy operation, in situ and real-time detection ability, high selectivity, and low cost [5, 6]. Many colorimetric and fluorescent sensors for H^+ and Cu^{2+} have been reported. However, most of them can only detect H^+ [7–12] or Cu^{2+} [13–19] individually. Previously, our group developed a sensor which could detect Cu^{2+} in CH_3CN/H_2O (1/1, v/v) and Fe^{3+} in CH_3CN/H_2O (1/99, v/v) [20]. Jo et al. [21], Gupta et al. [22], and Ozdemir [23] reported Cu^{2+} sensors that could also detect CN^-, Al(III), and Hg^{2+}, respectively. Recently, Fu et al. [24] reported a colorimetric and fluorescent sensor for Cu^{2+} and F^-. Some other works have described pH sensors that could also sense another ion, such as Zn^{2+}, Fe(III), or Bi^{3+} [25–27]. However, sensors that can respond to both H^+ and Cu^{2+}, especially using multiple channels in the same aqueous solution, are extremely rare [28].

In this work, we used 1,8-naphthalimide as chromophore and fluorophore, and hydrazine hydrate and furfural as receptor precursors to construct a new dye with simple structure and facile synthetic method. Moreover, the synergistic effects of N and O binding sites and their unique spatial locations enabled the dye to act as a spectral sensor which is highly selective to both H^+ and Cu^{2+} in the same aqueous medium using multiple signals and different mechanisms.

Experimental

Materials and instruments

All chemicals were obtained from commercial suppliers and used without further purification. Metal ions including K^+, Ca^{2+}, Na^+, Mg^{2+}, Fe^{2+}, Fe^{3+}, Cr^{3+}, Ag^+, Cd^{2+}, Co^{2+}, and Hg^{2+} were provided by their chloride salts, Zn^{2+}, Cu^{2+}, and Mn^{2+} were provided by their sulfate salts, and Pb^{2+} and Ni^{2+} were obtained from their acetate salts. These metal salts, *n*-butylamine, hydrazine hydrate ($NH_2NH_2{\cdot}H_2O$, 85%), and furfural (≥ 98%) were purchased from Sinopharm Chemical Reagent Co., Ltd. (Shanghai, China). 4-Bromine-1,8-naphthalic anhydride (98%) was provided by Anshan HIFI Chemical Co., Ltd.

^1H and ^{13}C nuclear magnetic resonance (NMR) were carried out on a UNITY Inova 400 spectrometer (Varian Co., USA). Absorption spectra were obtained on

a U-3900 spectrophotometer (PerkinElmer Co., USA). Fluorescence measurements were carried out using a F-2500 fluorescence spectrophotometer (Hitachi Co., Japan). Mass spectra were obtained on a Bruker micro-TOF-QIII spectrometer (Bruker Daltonics Co., Germany). Elemental analysis was carried out on a Carlo-Erba EA1110CHNO-S elemental analyzer (Carlo-Erba Co., Italy). pH values were tested using precise pH paper (Tzzt, Jiangsu). IR spectra were obtained using a MagNa-IR 550 spectrometer (Nicolet Co., USA).

Synthesis methods

The dye 2-*n*-butyl-6-(2-(furan-2-ylmethylene)hydrazinyl-1*H*-benzo[*de*]isoquinoline-1,3(2*H*)-dione (BNFA) was prepared by three-step reaction between 4-bromo-1,8-naphthalic anhydride, *n*-butylamine, hydrazine hydrate, and furfural, as shown in Scheme 1.

Synthesis of BBN [29]

4-Bromo-1,8-naphthalic anhydride (1.00 g, 3.62 mmol) was dispersed in 15 mL ethanol and heated to 50 °C. Then, *n*-butylamine (0.75 mL) was added. The mixture was stirred and refluxed for 24 h under nitrogen atmosphere. Subsequently, the reaction liquid was cooled to room temperature and poured into ice–water. Light-yellow precipitate appeared and was filtered and washed with water twice. The crude product was purified by recrystallization in ethanol to give the intermediate *N*-*n*-butyl-4-bromine-1,8-naphthalimide (BBN) as off-white needle crystal in 75.0% yield.

Synthesis of intermediate BNN [30]

Under nitrogen atmosphere, BBN (100 mg, 0.302 mmol) was dissolved in 10 mL ethylene glycol monomethyl ether and heated to 50 °C. Hydrazine hydrate (100 μL) was introduced. The reaction mixture was heated under reflux for 5 h, then cooled to room temperature and poured into distilled water. A solid was obtained by filtering and purified by washing with water (twice) and ethanol (once) to produce the intermediate 2-*n*-butyl-6-hydrazinyl-1*H*-benzo[*de*]isoquinoline-1,3(2*H*)-dione (BNN) as orange solid in 87.7% yield.

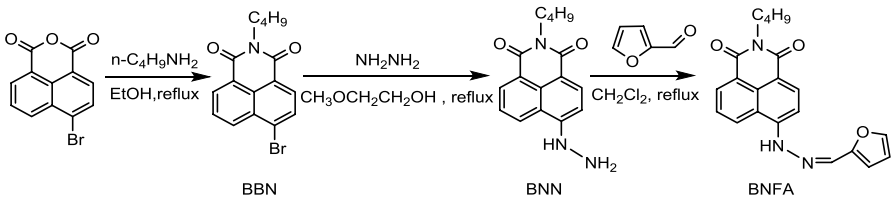

Scheme 1 Synthetic route of BNFA

Synthesis of BNFA

Under nitrogen atmosphere, 77 mg (0.27 mmol) BNN was dissolved in 15 mL dichloromethane and heated to 40 °C. Furfural (100 μL, 1.2 mmol) was added dropwise. The reaction mixture was stirred and refluxed for 5.5 h, then cooled to room temperature and filtered. Orange solid was obtained and purified by washing with water (twice) to give the dye BNFA in 67.9% yield. The structure of BNFA was fully characterized by IR, ^{1}H NMR, ^{13}C NMR, elemental analysis, and electrospray ionization (ESI) mass spectrometry (MS). IR (cm^{-1}) [Fig. S1 in Supporting Information (SI)]: 1110.97 (C–O–C), 1317.35 (C–N), 1554.50, 1578.89, 1536.37, 1616.79 (ArH), 1635.60 (C=O), 1681.89 (C=N), 2955.72, 2932.10, 2871.79 (CH_3, CH_2), 3279.95, 3454.43 (NH). ^{1}H NMR (400 MHz, DMSO-d_6) (Fig. S2 in SI), δ/ppm: 0.94 (t, 3H, J = 0.4 Hz), 1.35 (m, 2H), 1.60 (m, 2H), 4.00 (t, 2H, J = 3.6 Hz), 6.68 (q, 1H), 6.95 (d, 1H, J = 3.2 Hz), 7.57 (d, 1H, J = 8.4 Hz), 7.73 (t, 1H, J = 0.4 Hz), 7.88 (s, 1H), 8.31–8.34 (t, 2H, J = 1.6 Hz), 8.42 (d, 1H, J = 7.2 Hz), 8.68 (d, 1H, J = 8.4 Hz), 11.37 (s, 1H). ^{13}C NMR (400 MHz, DMSO-d_6) (Fig. S3 in SI), δ/ppm: 13.70, 19.79, 29.71, 39.04, 106.63, 110.90, 112.21, 112.46, 118.46, 121.86, 124.78, 127.99, 128.97, 130.64, 133.34, 133.85, 144.72, 146.07, 149.72, 162.95, 163.53. Elemental analysis data: Found C, 69.34; H, 5.42; N, 11.42%; Molecular formula $C_{21}H_{19}N_3O_3$ requires C, 69.79; H, 5.30; N, 11.63%. ESI–MS, Found (Fig. S4 in SI): $[M + H]^+$ 362.1541, $[M + Na]^+$ 384.1330; Molecular formula $C_{21}H_{19}N_3O_3$ requires $[M + H]^+$ 362.1505, $[M + Na]^+$ 384.1324.

Testing and calculation methods

General methods

Stock solution of BNFA (1×10^{-3} M) was prepared in CH_3CN. Stock solutions of metal salts (Ca^{2+}, K^+, Ni^{2+}, Fe^{3+}, Na^+, Fe^{2+}, Mg^{2+}, Ag^+, Mn^{2+}, Zn^{2+}, Hg^{2+}, Cr^{3+}, Pb^{2+}, Co^{2+}, Cd^{2+}, and Cu^{2+}) and ethylenediaminetetraacetic acid (EDTA) were prepared in deionized water (1×10^{-2} M). The tested solutions of BNFA, Cu^{2+} (or other metal ion), and their complex were prepared by mixing 0–100 μL stock solution of BNFA with 0–100 μL stock solution of Cu^{2+} (or other metal ion) in a volumetric flask (10 mL) and diluting to volume. The detection medium was CH_3CN/H_2O (1/1, v/v). H^+ concentration (pH) was adjusted using 0.1 M HCl and 0.1 M NaOH aqueous solutions. UV–Vis absorption and fluorescence spectra were recorded after standing for 1.5 h at 20 °C with excitation wavelength of 461 nm and slit width of 5 nm.

Detection limit

The detection limit was calculated as $3S/K$, where S is the standard deviation of five times of the blank measurement and K is the slope of the titration fit line [31].

Binding constant

The binding constant K was calculated using the Stern–Volmer Eq. (1) [32, 33], where F_0 and F are the fluorescent intensity at 558 nm before and after adding Cu^{2+}, $[Cu^{2+}]$ is the concentration of Cu^{2+}, and n is the binding stoichiometry for BNFA and Cu^{2+}.

$$\lg\left(\frac{F_0 - F}{F}\right) = n \lg\left[Cu^{2+}\right] + \lg K. \tag{1}$$

Results and discussion

Design and synthesis of dye

We used the well-known 1,8-naphthalimide as chromophore and fluorophore, and heteroatom-containing hydrazine hydrate and furfural as receptor precursors to prepare a new dye for cation sensing. All reactions in the synthesis were carried out under very mild conditions and offered good yields. Except for BBN (purified by recrystallization in ethanol), other intermediates and the dye could be obtained by succinct washing with water or ethanol. Hence, the dye can be obtained with high efficiency.

Spectra of BNFA at different pH values

In view of the pH sensitivity of the NH group, UV–Vis absorption and fluorescence spectra of BNFA in CH_3CN/H_2O (1/1, v/v) (initial pH 5.2) within the pH range of 1.9–12.0 were investigated. The results showed that the spectra were negligibly affected by pH from 1.9 to 5.2 (Fig. 1). When the pH was increased from 5.2 to 12.0, the absorbance at 461 nm and the fluorescence of the BNFA solution reduced, while

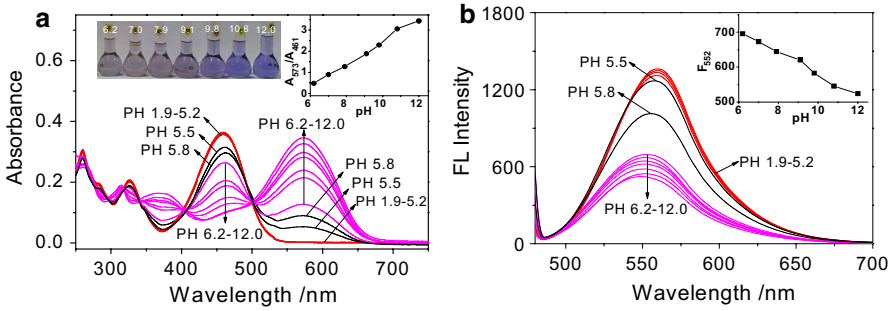

Fig. 1 UV–Vis absorption (**a**) and fluorescence (**b**) spectra of BNFA (10 μM) at different pH values. Solvent: CH_3CN/H_2O (1/1, v/v). λ_{ex}: 461 nm, slit width: 5 nm. pH: 1.9, 3.1, 4.0, 5.2, 6.2, 7.0, 7.9, 9.1, 9.8, 10.8, 12.0. Inset: color changes, as well as the relationship between A_{573}/A_{461} (or F_{552}) and pH. (Color figure online)

the absorbance at 573 nm increased gradually, accompanied by a change in the color of the solution from shallow purple to deep purple, which could be observed by naked eye. Moreover, the ratios of absorbance at 573 and 461 nm (A_{573}/A_{461}) of the BNFA solution increased (Fig. 1a, inset) while the corresponding fluorescence intensity at 552 nm (F_{552}) decreased (Fig. 1b, inset) almost linearly from pH 6.2 to 12.0. The linear equations were $A_{573}/A_{461} = 0.5256 \times \text{pH} - 2.8137$ ($R = 0.9949$) and $F_{552} = 888.2454 - 30.7614 \times \text{pH}$ ($R = 0.9926$). Therefore, we selected BNFA to detect H^+ (pH) in CH_3CN/H_2O (1/1, v/v) from pH 6.2 to 12.0.

Sensing H^+ using BNFA

Anti-interference of BNFA for detecting H^+

To investigate the disturbance of the detection of H^+ due to common metal ions, one ion from among K^+, Na^+, Mg^{2+}, Ag^+, Zn^{2+}, Cr^{3+}, Cd^{2+}, Co^{2+}, Ni^{2+}, Mn^{2+}, Fe^{2+}, Fe^{3+}, Pb^{2+}, Hg^{2+}, Cu^{2+}, and Ca^{2+} (10 eq.) was added into the solution of BNFA at pH 6.2 and 10.8. As shown in Fig. 2, the competing ions showed trivial effects on the A_{573}/A_{461} and F_{552} values of the solution. Therefore, BNFA showed good anti-interference ability when detecting H^+.

Time response

The time response of BNFA to H^+ is shown in Fig. 3. Upon using NaOH aqueous solution to change the pH of the BNFA solution from 6.2 to 10.8, A_{573}/A_{461} quickly rose while F_{552} greatly dropped. After 33 min, they both remained almost unchanged. Therefore, BNFA could respond to H^+ with relatively fast speed.

Mechanism for sensing of H^+ using BNFA

To understand the mechanism for H^+ sensing by BNFA, the reversibility between pH 6.2 and 10.8 was investigated by adding NaOH and HCl aqueous solution alternately. The results showed that the detection of H^+ by BNFA was reversible (Fig. 4).

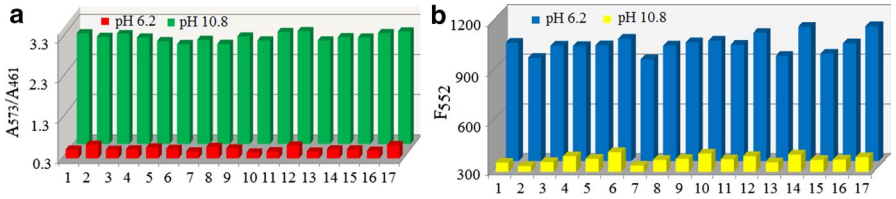

Fig. 2 Effects of coexisting ions on UV–Vis absorption (**a**) and fluorescence (**b**) maxima of BNFA for detecting H^+ in CH_3CN/H_2O (1/1, v/v). Concentration: 10 μM for BNFA, 100 μM for 2: Fe^{2+}, 3: Fe^{3+},4: Cu^{2+}, 5: Zn^{2+}, 6: Hg^{2+},7: Cr^{3+}, 8: Pb^{2+}, 9: Ca^{2+}; 10: Mg^{2+}, 11:Ag^+, 12: Na^+, 13: Co^{2+}, 14: Cd^{2+}, 15: Ni^{2+}, 16: K^+, 17: Mn^{2+}. 1: without coexisting ion. λ_{ex}: 461 nm, slit width: 5 nm. Red and green bar: A_{573}/A_{461} at pH 6.2 and pH 10.8. Blue and yellow bar: F_{552} at pH 6.2 and pH 10.8. (Color figure online)

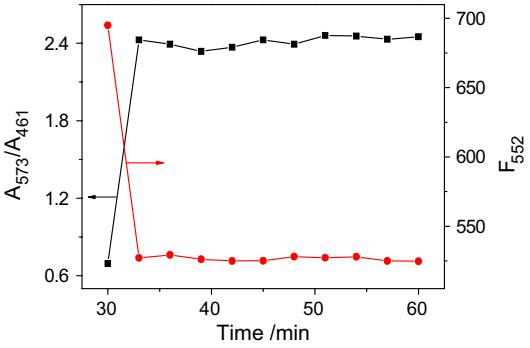

Fig. 3 Time response of BNFA to H^+. Solvent: CH_3CN/H_2O (1/1, v/v). Concentration: 10 μM for BNFA. λ_{ex}: 461 nm, slit width: 5 nm

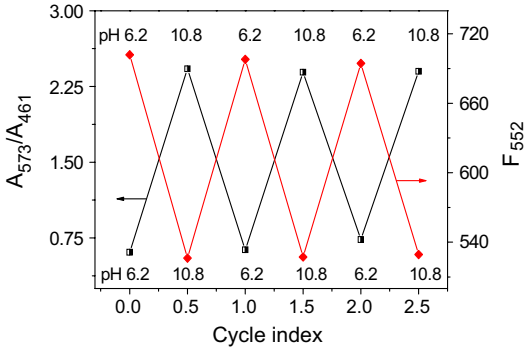

Fig. 4 Reversibility of ratiometric and fluorescent detection of H^+ with BNFA. Solvent: CH_3CN/H_2O (1/1, v/v); 10 μM for BNFA. λ_{ex}: 461 nm, slit width: 5 nm

Furthermore, ^{1}H NMR spectra of BNFA and BNFA–NaOH were collected in dimethylsulfoxide (DMSO)-d_6 (Fig. 5). Upon addition of 50 μL NaOH (0.1 M) into 600 μL DMSO-d_6 solution of BNFA (resulted in pH of 11.0), the peak at 11.38 ppm in the ^{1}H NMR spectrum of BNFA disappeared completely and the H peaks of the naphthalene ring varied. This can be explained based on the fact that OH^- trapped the H (j) in the NH linked to the naphthalene ring, resulting in changes of charge density and variation of the absorbance and fluorescence intensities of the BNFA solution.

Based on this reversibility, the ^{1}H NMR results, and literature [11, 34], we suggest a mechanism for H^+ sensing by BNFA in Scheme 2.

Detection of Cu^{2+} by BNFA

In the work described above, we used the pH sensitivity of BNFA in the range of pH 6.2–12.0 to monitor H^+. Thinking in other terms, its pH insensitivity would enable this sensor to detect analytes other than H^+ in multiple media at different pH values. Therefore, we further examined the spectral response of BNFA to metal ions in its insensitive pH range of 1.9–5.2. When 10 eq. of various metal cations such as Na^+, K^+, Ca^{2+}, Mg^{2+}, Fe^{2+}, Fe^{3+}, Mn^{2+},Cu^{2+}, Zn^{2+}, Cr^{3+}, Hg^{2+}, Pb^{2+}, Ni^{2+}, Ag^+, Cd^{2+}, and Co^{2+} was

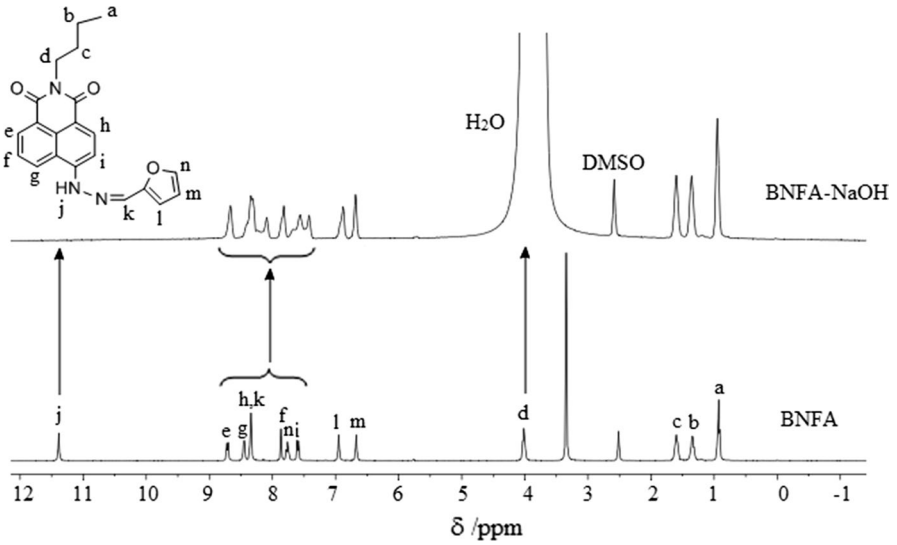

Fig. 5 ^{1}H NMR spectra of BNFA and BNFA–NaOH in DMSO-d_6 (400 MHz)

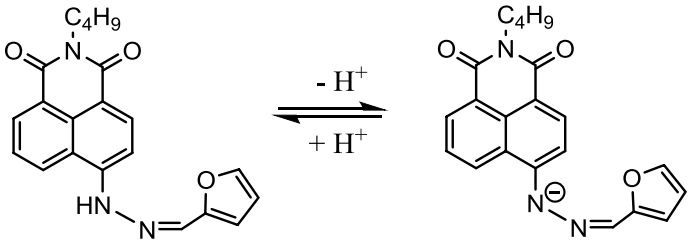

Scheme 2 Proposed H^+ sensing mechanism of BNFA

introduced into CH_3CN/H_2O (1/1, v/v) solution of BNFA (pH 5.2) individually, only Cu^{2+} induced a 4.6-fold decrease of the absorbance at 461 nm (A_{461}), accompanied by a color change from yellow to colorless observable to the naked eye, as shown in the UV–Vis absorption spectra (Fig. 6a). Similarly, only Cu^{2+} caused a 5.4-fold fall of the fluorescence intensity at 558 nm (F_{558}) accompanied by a 19-nm fluorescent blueshift and color change from orange to green (Fig. 6b). These results indicate that BNFA can be used as a triple-channel (UV–Vis absorption, fluorescence intensity reduction, as well as fluorescence blueshift) sensor for Cu^{2+} in CH_3CN/H_2O (1/1, v/v).

Anti-interference of BNFA for detecting Cu^{2+}

To investigate the disturbance from other coexisting metal ions on the detection of Cu^{2+} by BNFA, Cu^{2+} was added to CH_3CH/H_2O (1/1, v/v) solution of BNFA with

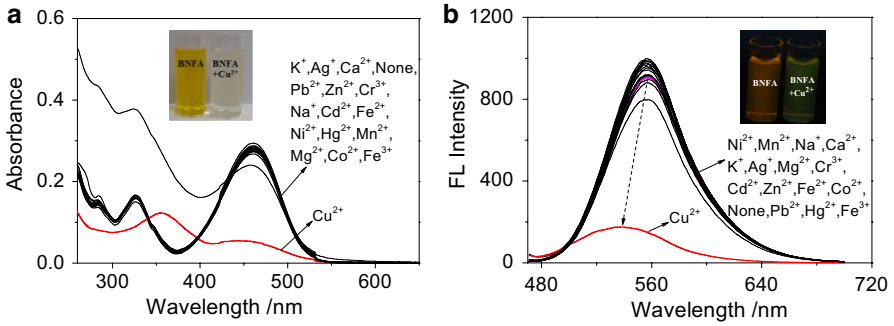

Fig. 6 UV–Vis absorption (**a**) and fluorescence (**b**) spectra as well as color change of BNFA in absence and presence of metal ions. Solvent: CH_3CN/H_2O (1/1, v/v), concentration: 10 μM for BNFA, 100 μM for metal ions. λ_{ex}: 461 nm, slit width: 5 nm

one metal ion from among K^+, Na^+, Mg^{2+}, Ag^+, Zn^{2+}, Cr^{3+}, Cd^{2+}, Co^{2+}, Ni^{2+}, Mn^{2+}, Fe^{2+}, Fe^{3+}, Pb^{2+}, Hg^{2+}, and Ca^{2+}. As shown in Fig. 7, Cu^{2+} could still decrease the UV–Vis absorption (a) and fluorescence (b) maxima remarkably. Therefore, BNFA exhibited good anti-interference performance in detection of Cu^{2+}.

Dependence of BNFA's spectra on Cu^{2+} concentration

To investigate whether BNFA could detect Cu^{2+} quantitatively, titration experiments were performed. As shown in Fig. 8, A_{461} of BNFA in CH_3CN/H_2O (1/1, v/v) gradually decreased with increase of the Cu^{2+} concentration ($[Cu^{2+}]$). When $[Cu^{2+}]$ reached 30 μM, A_{461} exhibited a stable trend. Moreover, A_{461} and $[Cu^{2+}]$ exhibited a good linear relationship with concentration in the range of 0–6 μM ($A_{461} = -0.02493 \times [Cu^{2+}] + 0.2475$, $R = 0.9713$). The fluorescence spectra of BNFA exhibited behavior similar to the UV–Vis absorption spectra, with $F_{558} = -144.5071 \times [Cu^{2+}] + 1280.6929$ ($R = 0.9625$). The detection limits evaluated by colorimetric and fluorescent titration were 6.10×10^{-7} and 2.62×10^{-7} M, respectively.

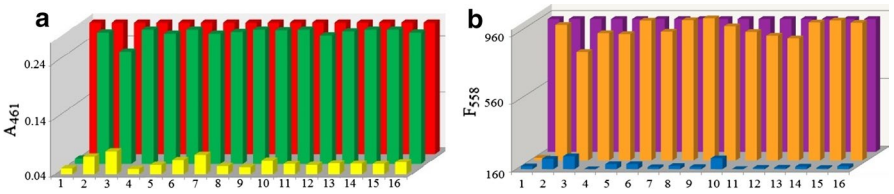

Fig. 7 Effects of coexisting ions (M^{n+}) on UV–Vis absorption (**a**) and fluorescence (**b**) maxima of BNFA–Cu^{2+} in CH_3CN/H_2O (1/1, v/v). Concentration: 10 μM for BNFA, 100 μM for 1: Cu^{2+}, 4: Zn^{2+}, 5: Hg^{2+}, 6: Cr^{3+}, 8: Ca^{2+}; 9: Mg^{2+}, 10: Ag^+, 11: Na^+, 12: Co^{2+}, 13: Cd^{2+}, 14: Ni^{2+}, 15: K^+, 16: Mn^{2+}. 50 μM for 2: Fe^{2+}, 3: Fe^{3+}, 7: Pb^{2+}. Red, green, and yellow bar: A_{461} of BNFA, BNFA–M^{n+}, and BNFA–M^{n+}–Cu^{2+}, respectively; Purple, orange, and blue bar: F_{558} of BNFA, BNFA–M^{n+}, and BNFA–M^{n+}–Cu^{2+}, respectively. λ_{ex}: 461 nm, slit width: 5 nm. (Color figure online)

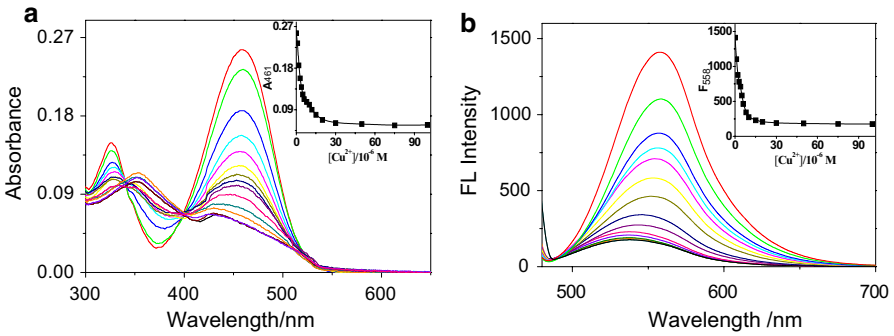

Fig. 8 UV–Vis absorption (**a**) and fluorescence (**b**) spectra of BNFA (10 μM) with various concentration of Cu^{2+}. Solvent: CH_3CN/H_2O (1/1, v/v). λ_{ex}: 461 nm, slit width: 5 nm. From top to bottom, concentration of Cu^{2+}: 0, 1, 2, 3, 4, 5, 6, 8, 10, 15, 20, 30, 50, 75, 100 μM. Inset: relationship between A_{461} (or F_{558}) and concentration of Cu^{2+}

Effect of pH

We also studied the effect of pH on the UV–Vis absorption and fluorescence spectra of BNFA–Cu^{2+} solution in the pH range of 1.9–5.2 (Fig. 9). Compared with that of BNFA solution (data from Fig. 1a), A_{461} and F_{558} of BNFA–Cu^{2+} solution were at very low level, and the absorbance (or fluorescence intensity) deviation between BNFA–Cu^{2+} and BNFA solutions was remarkable and stable. Therefore, BNFA could detect Cu^{2+} sensitively and reliably in the pH range of 1.9–5.2.

Time response

With the extension of time, A_{461} and F_{558} gradually reduced, then remained almost stable after about 60 min (Fig. 10). Therefore, BNFA could test Cu^{2+} with acceptable speed and good reliability.

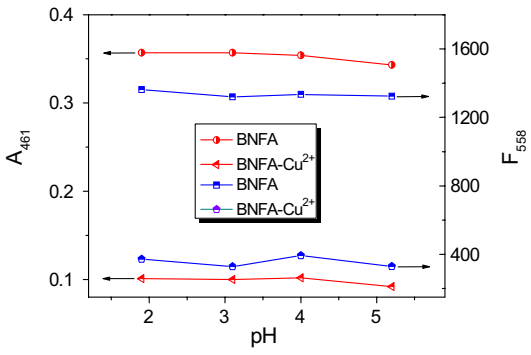

Fig. 9 Effect of pH on UV–Vis absorption at 461 nm and fluorescence intensity at 558 nm of BNFA and BNFA–Cu^{2+} in CH_3CN/H_2O (1/1, v/v). Concentration: 10 μM for BNFA, 100 μM for Cu^{2+}. pH: 1.9, 3.1, 4.0, 5.2

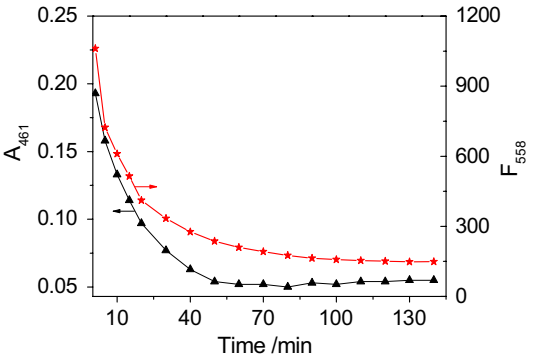

Fig. 10 Effect of time on UV–Vis absorption at 461 nm and fluorescence intensity at 558 nm of BNFA (10 μM)–Cu^{2+}(100 μM) in CH_3CN/H_2O (1/1, v/v)

Table 1 Recovery of Cu^{2+} in pond water and tap water ($n = 3$)[a]

Sample	Cu^{2+} added (10^{-6} mol/L)	Cu^{2+} found (10^{-6} mol/L)	Recovery (%)	RSD[a] (%)
Pond water	4	3.78	94.5	4.4
	6	5.86	97.7	0.9
Tap water	4	3.94	98.5	0.8
	6	5.86	97.7	0.9

[a]Solvent: CH_3CN/H_2O (1/1, v/v), BNFA: 10 μM, RSD: relative standard deviation

Practicability

Further, different concentrations of Cu^{2+} were added to tap water and pool water to examine the practicability of BNFA using our proposed fluorescence assay method. The data in Table 1 show that the concentrations of Cu^{2+} measured and added were indeed similar, with recovery values between 94.5 and 98.5%. The relative standard deviation (RSD) of three measurements was less than 4.4%. Therefore, BNFA can be used to detect Cu^{2+} in environmental water samples effectively.

Mechanism for Cu^{2+} sensing by BNFA

To explore the mechanism of Cu^{2+} sensing by BNFA, a Job's plot experiment was performed (Fig. 11). The total concentration of BNFA and Cu^{2+} was kept constant at 50 μM, while the molar fraction of Cu^{2+} was changed from 0.0 to 1.0. The maximal increment of the fluorescence intensity between BNFA and BNFA–Cu^{2+} appeared at 0.5 (Cu^{2+} molar fraction), indicating 1:1 stoichiometry between BNFA and Cu^{2+}. Based on this 1:1 binding mode and the fluorescence titration results, the binding constant calculated using the Stern–Volmer equation was $3.27 \times 10^4\ M^{-1}$.

Furthermore, reversibility was studied by adding EDTA into BNFA–Cu^{2+} solution. As shown in Fig. 12, the absorbance and fluorescence of BNFA–Cu^{2+} in CH_3CN/H_2O (1/1, v/v) could not be recovered by addition of excess EDTA, revealing that the reaction of BNFA with Cu^{2+} was irreversible.

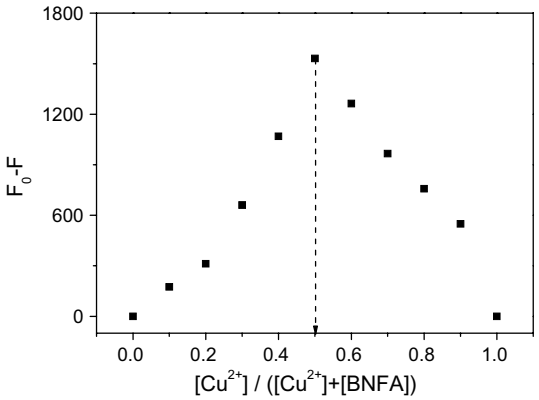

Fig. 11 Job's plot for Cu^{2+} versus BNFA. Total concentration ([BNFA] + [Cu^{2+}]): 50 μM. F_0 and F: fluorescence maxima at 558 nm before and after addition of Cu^{2+}, respectively. λ_{ex}: 461 nm, slit width: 5 nm

On the basis of the Job's plot, reversibility experiments, and literature [18, 35], a possible model for binding of BNFA with Cu^{2+} is proposed in Scheme 3. When Cu^{2+} meets BNFA in CH_3CN/H_2O (1/1, v/v), it first bonds via the N and O atoms of the moieties linked in C_4 of the naphthalene ring ($BNFA_1$), inducing intramolecular charge transfer (ICT), which results in cleavage of the C_4–N bond to form $BNFA_2$.

To validate the mechanism, liquid chromatography (LC)–MS spectra of BNFA–Cu^{2+} were recorded 30 min and 2 h after Cu^{2+} was added (Fig. 13). The peaks at *m/z* values of 447.4988, 362.1410, and 276.1903 in Fig. 13a can be ascribed to $[BNFA_1 + Na]^+$, $[BNFA + H]^+$, and $[BNFA_2 + Na]^+$, respectively. Meanwhile, Fig. 13b shows *m/z* peaks at 254.1100, 362.1499, and 384.1314, which correspond to $[BNFA_2 + H]^+$, $[BNFA + H]^+$, and $[BNFA + Na]^+$, respectively. These results basically support the mechanism proposed above.

To further verify the generation of $BNFA_2$ in the sensing process, 2 mg BNFA was reacted with 2 mg $CuSO_4{\cdot}5H_2O$ in 10 mL CH_3CN/H_2O (1/1, v/v) at 20 °C for 4 h. The resulting off-white precipitate was isolated by filtration, and its LC–MS spectrum was collected. As shown in Fig. 14, the peaks at *m/z* values of 254.1174

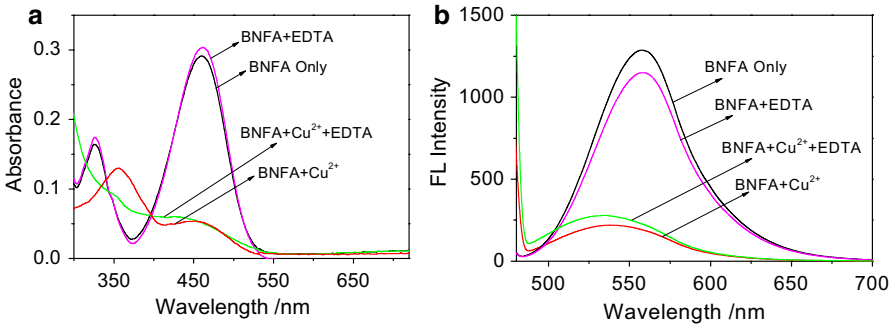

Fig. 12 Reversibility of absorbance (**a**) and fluorescent (**b**) detection of Cu^{2+} (100 μM) with BNFA (10 μM) in CH_3CN/H_2O (1/1, v/v). EDTA: 500 μM. λ_{ex}: 461 nm, slit width: 5 nm

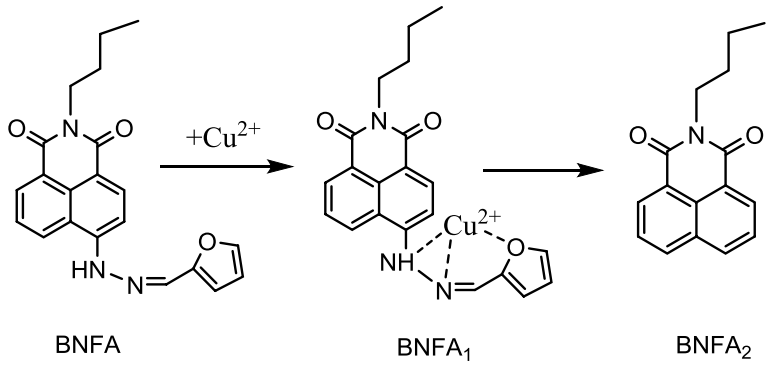

Scheme 3 Proposed Cu^{2+} sensing mechanism of BNFA

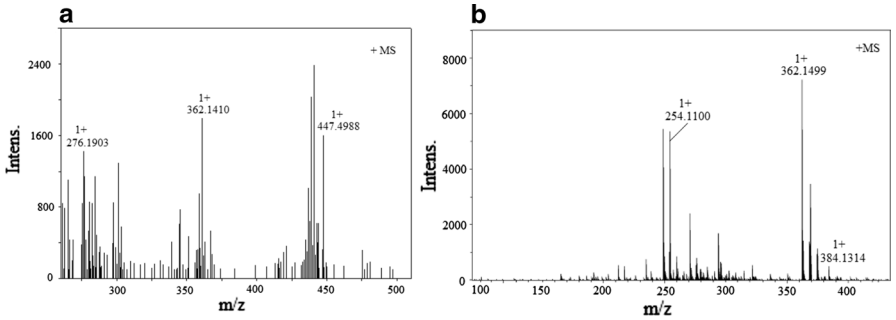

Fig. 13 LC–MS of BNFA at 30 min (**a**) and 2 h (**b**) after adding Cu^{2+}

and 276.0994 exactly match with the $[M + H]^+$ and $[M + Na]^+$ molecular ion peaks of $BNFA_2$, respectively. This result clearly confirms the validity of the sensing mechanism suggested above.

Conclusions

We report a novel, multifunction, multichannel 1,8-naphthalimide-based spectral sensor with simple structure and facile synthetic method. In CH_3CN/H_2O (1/1, v/v), BNFA was highly selective and sensitive for Cu^{2+} using triple channels in the pH range of 1.9–5.2, while it responded effectively to H^+ using dual channels within the pH range of 6.2–12.0. Its detection performance remained almost undisturbed by diverse coexistent ions. The H^+ sensing results from reversible transformation between N^- and NH at C-4 position of naphthalene ring. In contrast, the Cu^{2+} sensing can be explained based on the fact that Cu^{2+} first bonds to the two N atoms and one O atom of the receptor located in C-4 position of naphthalene ring, followed by irreversible cleavage of the complex.

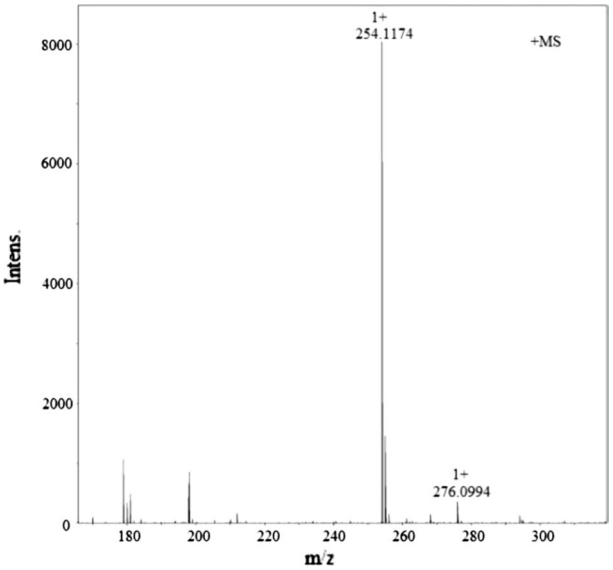

Fig. 14 LC–MS of product of reaction of BNFA and $CuSO_4 \cdot 5H_2O$

Acknowledgements This work was supported by the National Natural Science Foundation of China (21074085), Priority Academic Program Development of Jiangsu Higher Education Institutions, and State and Local Joint Engineering Laboratory for Novel Functional Polymeric Materials.

References

1. J.O. Carvalho, J.F.F. Orlanda, Food Chem. **233**, 159 (2017)
2. L. Mikulu, R. Michalicova, V. Iglesias, M.A. Yawer, A.E. Kaifer, P. Lubal, V. Sindelar, Chem. Eur. J. **23**, 2350 (2017)
3. D.B. Senn, S.B. Griscom, C.G. Lewis, J.P. Galvin, Environ. Sci. Technol. **38**, 3381 (2004)
4. J.H. Viles, Coordin. Chem. Rev. **256**, 2271 (2012)
5. J. Wu, W. Liu, J. Ge, H. Zhang, P. Wang, Chem. Soc. Rev. **40**, 3483 (2011)
6. X. Chen, T. Pradhan, F. Wang, J.S. Kim, J. Yoon, Chem. Rev. **112**, 1910 (2012)
7. A. Liu, M. Hong, W. Yang, S. Lu, D. Xu, Tetrahedron **70**, 6974 (2014)
8. E. Teknikel, C. Unalerogl, Dyes Pigments **120**, 239 (2015)
9. Z. Li, L. Li, T. Sun, L. Liu, Dyes Pigments **128**, 165 (2016)
10. C. Sha, Y. Chen, Y. Chen, D. Xu, J. Fluoresc. **26**, 1709 (2016)
11. N.I. Georgiev, M.D. Dimitrova, P.V. Krasteva, V.B. Bojinov, J. Lumin. **187**, 383 (2017)
12. S. Radunz, H.R. Tschiche, D. Moldenhauer, U.R. Genger, Sens. Actuators B Chem. **251**, 490 (2017)
13. T.S. Reddy, A.R. Reddy, Spectrochim. Acta Part A **128**, 880 (2014)
14. S. Pu, L. Ma, G. Liu, H. Ding, B. Chen, Dyes Pigments **113**, 70 (2015)
15. C. Li, K. Xiang, Y. Liu, Y. Zheng, L. Pan, B. Tian, J. Zhang, Res. Chem. Intermed. **41**, 5915 (2015)
16. A.N. Kursunlu, E. Sahin, E. Güler, J. Fluoresc. **26**, 1997 (2016)
17. G. He, Q. Meng, X. Zhao, C. He, P. Zhou, C. Duan, Inorg. Chem. Commun. **65**, 28 (2016)
18. X. Hua, X. Zheng, X. Fan, Y. Su, X. Zhan, Sens. Actuators B Chem. **227**, 191 (2016)
19. I.J. Chang, M.G. Choi, Y.A. Jeong, S.H. Lee, S.K. Chang, Tetrahedron Lett. **58**, 474 (2017)
20. A. Liu, L. Yang, Z. Zhang, Z. Zhang, D. Xu, Dyes Pigments **99**, 472 (2013)
21. H.Y. Jo, G.J. Park, Y.J. Na, Y.W. Choi, G.R. You, C. Kim, Dyes Pigments **109**, 127 (2014)
22. V.K. Gupta, N. Mergu, L.K. Kumawat, Sens. Actuators B Chem. **223**, 101 (2016)

23. M. Ozdemir, J. Photochem. Photobiol. A **318**, 7 (2016)
24. Y. Fu, C. Fan, G. Liu, S. Pu, Sens. Actuators B Chem. **239**, 295 (2017)
25. S.M. Dimov, N.I. Georgiev, A. Asiri, V.B. Bojinov, J. Fluoresc. **24**, 1621 (2014)
26. C. Hua, H. Zheng, K. Zhang, M. Xin, J. Gao, Y. Li, Tetrahedron **72**, 8365 (2016)
27. R. Kavitha, T. Stalin, Sens. Actuators B Chem. **247**, 632 (2017)
28. L. Xu, S. Wei, Q. Diao, P. Ma, X. Liu, X. Wang, Sens. Actuators B Chem. **246**, 395 (2017)
29. L. Kang, Z. Xing, X. Ma, Y. Liu, Spectrochim. Acta Part A **167**, 59 (2016)
30. Z. Chen, L. Wang, G. Zou, J. Tang, X. Cai, M. Teng, Spectrochim. Acta Part A **105**, 57 (2013)
31. K. Karaoglu, F. Yilmaz, E. Menteşe, J. Fluoresc. **27**, 1293 (2017)
32. J. Xiao, X. Chen, L. Zhang, S.G. Talbot, G.C. Li, M. Xu, J. Agric. Food Chem. **56**, 910 (2008)
33. E. Gökoğlu, E. Yılmaz, J. Fluoresc. **24**, 1439 (2014)
34. Y. Fu, J. Zhang, H. Wang, J. Chen, G. Chen, X. He, Dyes Pigments **133**, 372 (2016)
35. C. Liu, J. Xu, F. Yang, W. Zhou, Z. Li, L. Wei, Sens. Actuators B Chem. **212**, 364 (2015)